Di-tert-butyldiphosphatetrahedrane as a Source of 1,2-Diphosphacyclobutadiene Ligands

Hierlmeier, G.; Coburger, P.; Scott, D.J.; Maier, T.M.; Pelties, S.; Wolf, R.; Pividori, D.M.; Meyer, K.; van Leest, N.P.; de Bruin, B.

DOI
10.1002/chem.202102335

Publication date
2021

Document Version
Final published version

Published in
Chemistry-A European Journal

Full Paper
doi.org/10.1002/chem.202102335

Chemistry Europe
European Chemical Societies Publishing

Di-*tert*-butyldiphosphatetrahedrane as a Source of 1,2-Diphosphacyclobutadiene Ligands

Gabriele Hierlmeier,[a] Peter Coburger,[a, b] Daniel J. Scott,[a] Thomas M. Maier,[a] Stefan Pelties,[a] Robert Wolf,*[a] Daniel M. Pividori,[c] Karsten Meyer,[c] Nicolaas P. van Leest,[d] and Bas de Bruin[d]

Abstract: Reactions of di-*tert*-butyldiphosphatetrahedrane (**1**) with cycloocta-1,5-diene- or anthracene-stabilised metalate anions of iron and cobalt consistently afford complexes of the rarely encountered 1,2-diphosphacyclobutadiene ligand, which have previously been very challenging synthetic targets. The subsequent reactivity of 1,2-diphosphacyclobutadiene cobaltates toward various electrophiles has also been investigated and is compared to reactions of related 1,3-diphosphacyclobutadiene complexes. The results highlight the distinct reactivity of such isomeric species, showing that the 1,2-isomers can act as precursors for previously unknown triphospholium ligands. The electronic structures of the new complexes were investigated by several methods, including NMR, EPR and Mößbauer spectroscopies as well as quantum chemical calculations.

Introduction

Tetrahedranes are highly strained derivatives of the simplest platonic hydrocarbon C_4H_4.[1] The first isolated tetrahedrane was undoubtedly white phosphorus, P_4, first prepared in the 17th century. Much more recently (1978), the group of Maier showed that the carbon-based tetrahedrane tBu_4C_4 can be accessed as well.[2] Even though heavier group 14 tetrahedranes with various substituents have been prepared, mixed neutral tetrahedranes have remained scarce.[3] This is especially conspicuous considering the great number of mixed anionic tetrahedranes containing group 13, 14 or 15 elements.[4] Our group recently showed that mixed group 14 / group 15 tetrahedranes are indeed accessible.[5] A simple nickel-catalysed dimerisation reaction of *t*BuCP affords the phosphaalkyne dimer di-*tert*-butyldiphosphatetrahedrane $(tBuCP)_2$ (**1**, Figure 1A), which can be considered a 'hybrid' between P_4 and $(tBuC)_4$. The related tri-*tert*-butylphosphatetrahedrane was reported shortly thereafter by Cummins and co-workers.[6]

Having been synthetically inaccessible until recently, the reactivity of these phosphatetrahedranes is still largely unexplored, although preliminary results suggest that **1** possesses a versatile coordination chemistry. For example, **1** reacts with

[a] Dr. G. Hierlmeier, Dr. P. Coburger, Dr. D. J. Scott, Dr. T. M. Maier, Dr. S. Pelties, Prof. Dr. R. Wolf
Institut für Anorganische Chemie
Universität Regensburg
93040 Regensburg (Germany)
E-mail: robert.wolf@ur.de

[b] Dr. P. Coburger
present address:
Laboratory of Inorganic Chemistry
ETH Zürich
8093 Zürich (Switzerland)

[c] D. M. Pividori, Prof. Dr. K. Meyer
Institut für Anorganische Chemie
Friedrich-Alexander-Universität Erlangen-Nürnberg
Egerlandstraße 1, 91058 Erlangen (Germany)

[d] Dr. N. P. van Leest, Prof. Dr. B. de Bruin
Van 't Hoff Institute for Molecular Sciences
University of Amsterdam
Science Park 904 1098 XH Amsterdam (The Netherlands)

Supporting information for this article is available on the WWW under https://doi.org/10.1002/chem.202102335

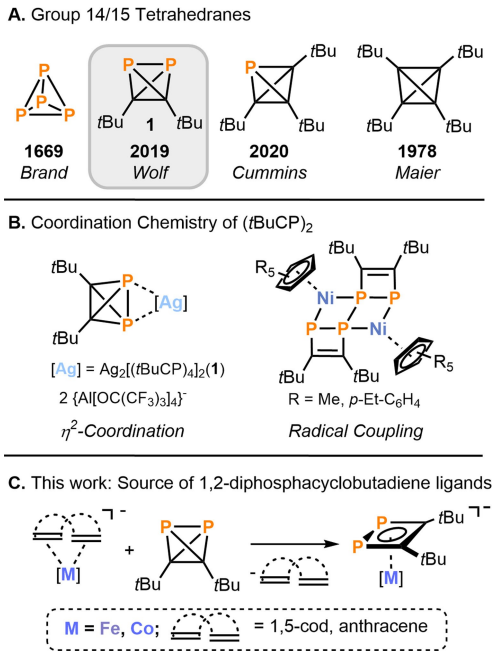

Figure 1. Group 14/15 tetrahedranes and coordination chemistry of $(tBuCP)_2$.

various Ni(0) and Ni(I) complexes to form (tBuCP)$_n$ (n = 2, 4) frameworks with novel coordination modes.[7] Moreover, it coordinates in an η^2-fashion via its lone pairs to silver(I) (Figure 1B).[5] Significantly, in this latter case the behaviour of **1** is noticeably different from that of either P_4 or the monomeric *tert*-butylphosphaalkyne, both of which react with Ag^+ cations to give homoleptic complexes $[AgL_2]^+$ (L = η^2-P_4, η^2-tBuCP).[8] Furthermore, in one of our most recent contributions, the reactivity of **1** towards carbenes was investigated.[9] This study highlighted that, while **1** appears to be reactive towards similar substrates as P_4 and tBuCP, these reactions furnish distinctly different and otherwise inaccessible products.

Based on the above results, we were highly motivated to investigate the reactivity of **1** towards low-valent 3d metalates. The reactions of these species with P_4 have been extensively studied: for example, Ellis and Urnėžius were able to synthesise the first completely inorganic sandwich complex $[(\eta^5\text{-}P_5)_2Ti]^{2-}$ by reaction of a titanate with P_4.[10] Our group has also contributed to this area by reaction of alkene- or arene-stabilised cobaltates and ferrates with P_4.[11,12] Many of the same metalates are also known to react with tBuCP to give 1,3-diphosphacyclobutadiene complexes of the type $[M(1,3\text{-}R_2C_2P_2)_2]^-$ (M = Fe, Co; R = tBu, tPent, Ad) by head-to-tail cyclodimerisation of the phosphaalkyne.[13,14] These 1,3-tBu$_2$C$_2$P$_2$ complexes possess versatile coordination behaviour and display much other onward reactivity, and can be used to access a variety of other coordination compounds.[15] By analogy with our previous studies, it was anticipated that related reactions of metalates with **1** could provide access to similarly interesting and synthetically useful coordination complexes, that would not be accessible using established precursors.

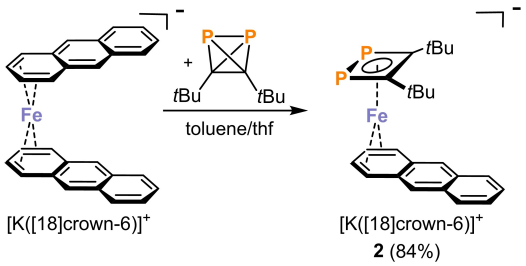

Scheme 1. Reaction of [K([18]crown-6)][Fe(anthracene)$_2$] with (tBuCP)$_2$.

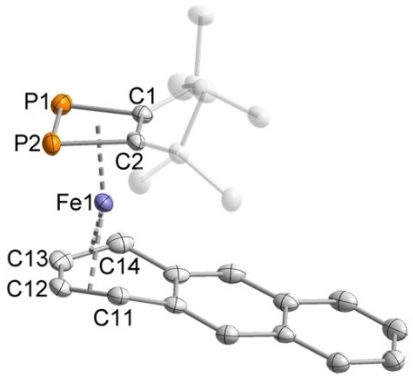

Figure 2. Molecular structure of [K([18]crown-6)][Fe(1,2-tBu$_2$C$_2$P$_2$)(anthracene)] (**2**) in the solid state (anion shown only).[31] Thermal ellipsoids are set at the 50% probability level. Hydrogen atoms and the $[K([18]crown\text{-}6)]^+$ cation are omitted for clarity. Selected bond lengths [Å] and angles [°]: P1–P2 2.1738(6), P1–C1 1.8328(15), P2–C2 1.8274(14), C1–C2 1.440(2), Fe–($C_2P_2^{centroid}$) 1.783(2), C11–C12 1.428(2), C12–C13 1.403(2), C13–C14 1.432(2), C1–P1–P2 78.03(5), C2–P2–P1 78.85(5), C2–C1–P1 101.97(10), C1–C2–P2 101.14(10).

Results and Discussion

Syntheses and molecular structures

To begin, the reaction of two equivalents of **1** with one equivalent of the anthracene ferrate [K([18]crown-6)][Fe(anthracene)$_2$] in THF was studied. Addition of **1** to a dark red solution of [K([18]crown-6)][Fe(anthracene)$_2$] in THF at −80 °C afforded an intense green solution after stirring the reaction overnight, while allowing it to warm to room temperature. X-ray diffraction analysis on single crystals grown from benzene/*n*-hexane revealed the formation of the heteroleptic complex [K([18]crown-6)][Fe(1,2-tBu$_2$C$_2$P$_2$)(anthracene)] (**2**, Scheme 1, Figure 2). Notably, despite the 2:1 reaction stoichiometry, **2** was the only product isolated, with no observation of a homoleptic 2:1 complex. Thus, using an optimised protocol with 1:1 stoichiometry, **2** was isolated in good yields of up to 84% as a green powder. Compound **2** shows both a very rare η^4-coordinated 1,2-diphosphacyclobutadiene ligand and an η^4-coordinated anthracene ligand. The bond lengths in the tBu$_2$C$_2$P$_2$ ligand compare well to those reported previously for the related cobalt complex [Cp‴Co(1,2-tBu$_2$C$_2$P$_2$)] [**2**: P1–P2 2.1738(6) Å, C1–C2 1.440(2) Å; [Cp‴Co(1,2-tBu$_2$C$_2$P$_2$)]: P–P 2.1818(7) Å), C–C 1.443(2) Å; Cp‴ = 1,2,4-tBu$_3$C$_5$H$_2$)],[16] while the bond lengths within the anthracene ligand (C11–C12 1.428(2) Å, C12–C13 1.403(2) Å, C13–C14 1.432(2) Å) indicate back donation from an Fe(I) to the π-system of the ligand. Notably, 1,2-diphosphacyclobutadiene ligands are very rare compared to their 1,3-isomers, which are commonly prepared by dimerisation of phosphaalkynes in the coordination sphere of transition metals.[16,17] Hence, the formation of complex **2** suggested a distinct synthetic utility of **1** in the synthesis of 1,2-diphosphacyclobutadiene complexes, for which no reliable, general synthetic routes have previously been available (see below). Notably, attempts to isolate the isomer [Fe(1,3-tBu$_2$C$_2$P$_2$)(anthracene)]$^-$ from the reaction of two equivalents of tBuCP and [K([18]crown-6)][Fe(anthracene)$_2$] have not been successful so far.

Complex **2** was characterised by UV/Vis spectroscopy, showing an intense absorption band at 650 nm, which accounts for its green colour. The complex is paramagnetic with an effective magnetic moment of μ_{eff} = 1.9(1) μ_B determined by the Evans NMR method. As a result of the paramagnetism, the ^{1}H NMR spectrum of isolated **2** in THF-d$_8$ shows no signals except for the solvent signals in the range from −150 to 150 ppm. Further characterisation data, including the X-band EPR and zero-field ^{57}Fe Mössbauer spectra, are described in the section *Electronic Structure Analysis* (see below).

To test the generality of 1,2-diphosphacyclobutadiene formation, **1** was next reacted with the cobaltate $[K(thf)_{0.2}][Co(\eta^4\text{-}cod)_2]$ (cod = 1,5-cyclooctadiene). Addition of two equivalents of **1** to a THF solution at −80 °C led to the formation of an orange-brown solution. The $^{31}P\{^1H\}$ NMR spectrum of the reaction mixture showed two major singlet species with chemical shifts of −102.3 and 3.3 ppm in a 5:1 ratio (integration). The latter, minor shift is close to the reported value for $[K([18]crown\text{-}6)(thf)_2][Co(1,3\text{-}tBu_2C_2P_2)_2]$ (δ = 2.4 ppm).[13] Indeed, extraction of the crude reaction mixture with 1,4-dioxane and slow diffusion of *n*-hexane afforded yellow crystals of both a 1,4-dioxane solvated salt of the previously reported cobaltate $[Co(1,3\text{-}tBu_2C_2P_2)_2]^-$ (**3'**) and the new, isomeric complex $[K([18]crown\text{-}6)(1,4\text{-}dioxane)_4][Co(1,2\text{-}tBu_2C_2P_2)_2]$ (**3**), containing a 1,2-diphosphacyclobutadiene ligand (Scheme 2).[13] The 'mixed' isomer containing both 1,2- and 1,3-diphospacyclobutadiene ligands is not observed, which is attributed to increased steric repulsion between the *t*Bu groups in this isomer, as discussed in the computational details (see the Supporting Information). Again, these results highlight both the divergent reactivity of **1** and *t*BuCP (whose reactions with $[K(thf)_{0.2}][Co(\eta^4\text{-}cod)_2]$ preferentially form the 1,2-isomer **3** and the 1,3-isomer **3'**, respectively), and the ability of **1** to act as a 1,2-diphosphacyclobutadiene ligand precursor.

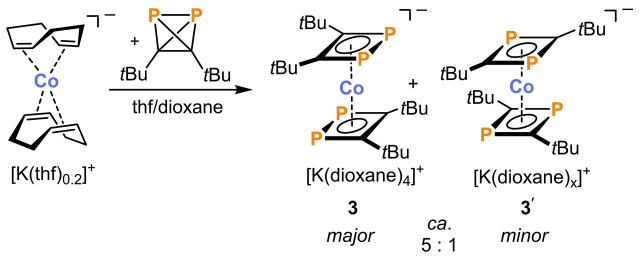

Scheme 2. Reaction of $[K(thf)_{0.2}][Co(\eta^4\text{-}cod)_2]$ with $(t\text{BuCP})_2$.

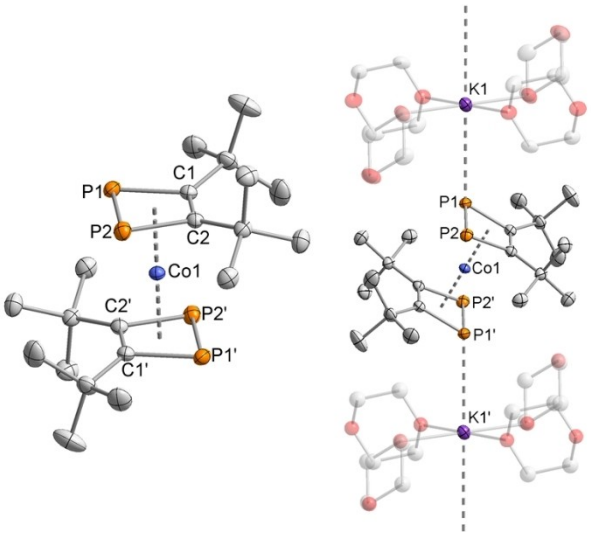

Figure 3. Molecular structure of **3** (left: anion shown only, right: structure as coordination polymer) in the solid state.[31] Thermal ellipsoids are set at the 50% probability level. Hydrogen atoms are omitted for clarity. Selected bond lengths [Å] and angles [°]: P1–P2 2.1798(6), P1–C1 1.8234(17), P2–C2 1.8136(17), C1–C2 1.443(2), K1–P1 3.4898(5), Co – ($C_2P_2^{centroid}$) 1.748(2), C1–P1–P2 78.26(6), C2–P2–P1 78.36(6), C2–C1–P1 101.39(12), C1–C2–P2 102.00(11).

The solid-state molecular structure of **3** revealed a polymer built upon coordination of the 1,2-diphosphacyclobutadiene ligands to $[K(1,4\text{-dioxane})_4]^+$ units (Figure 3). The P–P bond length of 2.1798(6) Å and the C1–C2 bond length (1.443(2) Å) of the diphosphacyclobutadiene ligand compare well to **2**, as well as to the Co complex $[Cp'''Co(1,2\text{-}tBu_2C_2P_2)]$ mentioned above. The two η^4-bound $tBu_2C_2P_2$ units are in a staggered conformation with the *t*Bu groups pointing away from each other. Due to very similar solubilities, **3** could not be separated from **3'**. Moreover, heating the crude reaction mixture to 110 °C for several days did not change the integral ratio of the signals for **3** and **3'** in the $^{31}P\{^1H\}$ NMR spectrum; thus, showing that the two species do not convert into each other under these conditions. The reaction of $[K(thf)_{0.2}][Co(\eta^4\text{-}cod)_2]$ with just one equivalent of **1** also afforded the same mixture of homoleptic cobalt complexes in the $^{31}P\{^1H\}$ NMR spectrum (signals at −102.3 and 3.3 ppm) alongside unconsumed $[K(thf)_{0.2}][Co(\eta^4\text{-}cod)_2]$, as identified in the ^1H NMR spectrum.

To establish whether 1,2-diphosphacyclobutadiene ligand formation from **1** is a general phenomenon, reactions were next performed using the BIAN cobaltate $[K(thf)_{1.5}][(^{Dipp}BIAN)Co(\eta^4\text{-}cod)]$ (BIAN = bis(aryl)acenaphthenequinonediimine, Dipp = 2,6-di-*iso*-propylphenyl), whose reactions with P_4 have previously been shown to proceed with particularly high selectivity.[12] Addition of one equivalent of **1** to a dark green solution of $[K(thf)_{1.5}][(^{Dipp}BIAN)Co(\eta^4\text{-}cod)]$ resulted in a colour change to turquoise overnight. Reaction monitoring by $^{31}P\{^1H\}$ NMR spectroscopy revealed full consumption of **1** after stirring the reaction for 3 days at ambient temperature. Gratifyingly, the selective formation of one species with a singlet resonance at a chemical shift of −121.8 ppm was observed. Single crystal X-ray diffraction studies on crystals grown from 1,4-dioxane/*n*-hexane revealed the formation of the heteroleptic 1,2-diphosphacyclobutadiene complex $[K(1,4\text{-dioxane})][(^{Dipp}BIAN)Co(1,2\text{-}tBu_2C_2P_2)]$ (**4**, Scheme 3, Figure 4). In the solid state, each K^+ counterion is coordinated by the two P atoms of one anion, the Dipp substituent of another anion and a 1,4-dioxane molecule, resulting in a dimeric structure (see Figure S33). The bond metrical parameters of the 1,2-$tBu_2C_2P_2$ ligand resemble the data obtained for **2** and **3**. While the C–C bond length (1.403(3) Å) is in good agreement with a dianionic $^{Dipp}BIAN^{2-}$ ligand (1.402(4) Å in $Na_2{}^{Dipp}BIAN$), the N1–C11 (1.353(3) Å) and N2–C12 (1.347(3) Å) bond lengths deviate slightly from the reported values of 1.387(4) and 1.386(4) Å.[19] A more detailed analysis of the bond metric data of the BIAN ligands will be discussed below (section on *Electronic Structure Analysis*).

Compound **4** was isolated in 63% crystalline yield and fully characterised by NMR and UV/Vis spectroscopies as well as elemental analysis. The ^1H and $^{13}C\{^1H\}$ NMR spectra of **4** reveal a diamagnetic compound with one signal set for the $^{Dipp}BIAN$ and one signal set for the $tBu_2C_2P_2$ ligand. The $^{31}P\{^1H\}$ NMR spectrum shows a singlet resonance at −121.8 ppm, which is comparable

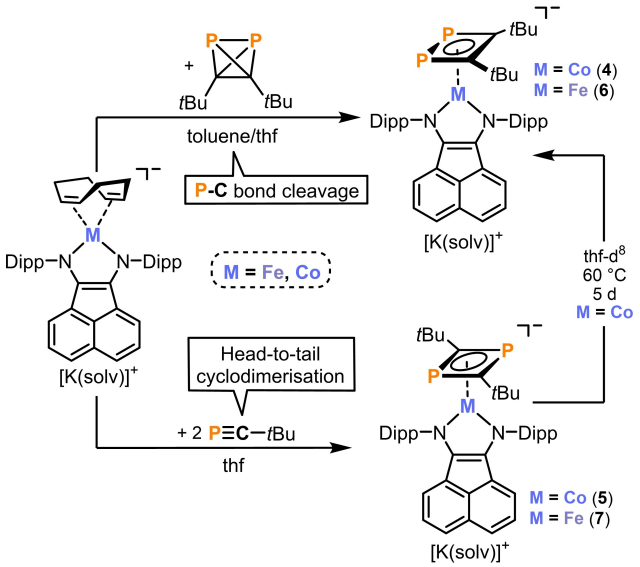

Scheme 3. Synthesis of heteroleptic [K(solv)][(^{Dipp}BIAN)M(tBu$_2$C$_2$P$_2$)] (M = Co, Fe) complexes featuring 1,2- or 1,3-(tBu$_2$C$_2$P$_2$) ligands. [K(solv)]$^+$ observed in the molecular structure determined by XRD: [K(1,4-dioxane)]$^+$ (**4**), [K(thf)$_3$]$^+$ (**5**), [K([18]crown-6)(1,4-dioxane)]$^+$ (**6**), [K([18]crown-6)(thf)$_{1.8}$(1,4-dioxane)$_{0.2}$]$^+$ (**7**). [K(solv)]$^+$ for starting materials: [K(thf)$_{1.5}$] (M = Co), [K([18]crown-6)] (M = Fe).

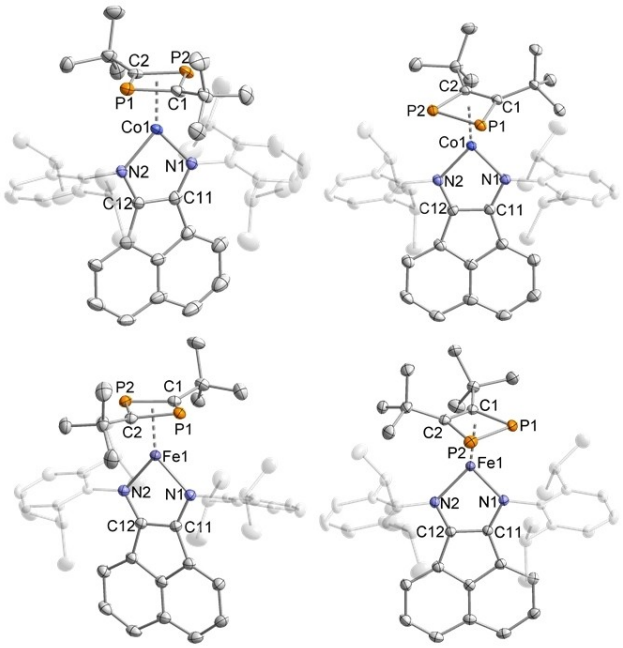

Figure 4. Molecular structures of **4**–**7** in the solid state.[31] Thermal ellipsoids are set at the 50% probability level. Hydrogen atoms, cations (with sequestering agent [18]crown-6 in case of **6** and **7**) and solvent of crystallisation are omitted for clarity. For **5** and **6**, only one of two crystallographically independent molecules is shown. Selected bond lengths [Å] and angles [°]: **4**: P1–P2 2.1765(8), P1–C1 1.838(2), P2–C2 1.815(2), C1–C2 1.441(3), N1–C11 1.353(3), N2–C12 1.347(3), C12–C11 1.403(3), Co1–N1 1.9382(18), Co1–N2 1.9074(18), Co-(C_2P_2centroid) 1.775(2), C2–C1–P1 102.62(16), C1–C2–P2 100.60(16), C1–P1–P2 77.11(7), C2–P2–P1 79.66(8); **5**: P1–C1 1.802(4), P1–C2 1.787(5), P2–C1 1.787(4), P2–C2 1.802(4), N1–C11 1.358(6), N2–C12 1.352(5), C12–C11 1.397(6), Co1–N1 1.929(3), Co1–N2 1.909(4), Co-(C_2P_2centroid) 1.780(2), P2–C1–P1 98.4(2), P1–C2–P2 98.4(2), C2–P1–C1 81.45(19), C1–P2–C2 81.4(2).; **6**: P1–P2 2.173(5), P1–C1 1.819(9), P2–C2 1.776(10), C1–C2 1.434(13), N1–C11 1.369(9), N2–C12 1.350(9), C12–C11 1.413(10), Fe1–N1 1.959(6), Fe1–N2 1.958(7), Fe-(C_2P_2centroid) 1.823(3), C2–C1–P1 100.8(7), C1–C2–P2 103.0(7), C1–P1–P2 77.7(3), C2–P2–P1 78.5(3); **7**: P1–C1 1.799(2), P1–C2 1.795(2), P2–C1 1.790(2), P2–C2 1.791(2), N1–C11 1.367(3), N2–C12 1.366(2), C12–C11 1.385(3), Fe1–N1 1.9421(16), Fe1–N2 1.9331(17), Fe-(C_2P_2centroid) 1.803(3), P2–C1–P1 98.94(10), P2–C2–P1 99.01(10), C2–P1–C1 80.54(9), C1–P2–C2 80.89(10).

to **3** and to the complex [(Cp'''Co(1,2-tBu$_2$C$_2$P$_2$)] ($\delta(^{31}P\{^1H\}) = -83.8$ ppm).[16]

As noted previously, 1,3-diphosphacyclobutadiene complexes can be prepared by head-to-tail cyclodimerisation reactions. Indeed, the reaction of 2 equivalents of tBuC≡P with the same precursor [K(thf)$_{1.5}$][(^{Dipp}BIAN)Co(η^4-cod)] afforded the isomeric 1,3-diphosphacyclobutadiene complex [K(thf)$_3$][(^{Dipp}BIAN)Co(1,3-tBu$_2$C$_2$P$_2$)] (**5**) in 64% yield as turquoise crystals. The solid-state molecular structure of **5** shows chelation of the potassium cation by one P atom of the tBu$_2$C$_2$P$_2$ ring and the phenyl ring of the Dipp group in the same anion, resulting in a monomeric structure (in contrast to **4**). The P–C bond lengths in this complex lie in the range of 1.787(4) to 1.802(4) Å and the bond metric data of the BIAN ligand will be discussed below. In the $^{31}P\{^1H\}$ NMR spectrum one singlet at 1.8 ppm was observed. Compounds **4** and **5** represent rare examples of heteroleptic transition metalate anions with terminal 1,3-diphosphacyclobutadiene ligands.

The intense turquoise colouration of both **4** and **5** when dissolved in THF can be rationalised by their UV/Vis absorption spectra, with absorption bands at 630 nm (**4**) and 605 nm (**5**). When heating a solution of **5** in THF-d$_8$ for 5 days to 60 °C, the selective formation of **4** was observed. This is in line with a computational analysis on the stability of the truncated model complexes [(^{Dmp}BIAN)Co(1,2-tBu$_2$C$_2$P$_2$)]$^-$ and [(^{Dmp}BIAN)Co(1,3-tBu$_2$C$_2$P$_2$)]$^-$ (Dmp = 2,6-dimethylphenyl) at the RI-PWPB95-D3BJ/def2-TZVP level of theory. Although single point calculations using this double hybrid functional suggest little difference in energy between the isomers, the 1,2-diphosphacyclobutadiene is thermodynamically more stable than its 1,3-isomer (see the Supporting Information). A single related thermal isomerisation of a 1,3-diphosphacyclobutadiene ligand to its 1,2-isomer has been observed by Scheer and co-workers to generate [(Cp'''Co(1,2-tBu$_2$C$_2$P$_2$)].[16]

To probe whether these differences in reactivity could be further extended, the analogous ferrate [K([18]crown-6)][(^{Dipp}BIAN)Fe(η^4-cod)] was reacted with tBuCP and its dimer **1** (Scheme 3). Single crystals suitable for X-ray diffraction studies were obtained from both reactions, which confirmed the analogous formation of two isomeric products: [K([18]crown-6)(1,4-dioxane)][(^{Dipp}BIAN)Fe(1,2-tBu$_2$C$_2$P$_2$)] (**6**, from **1**) and [K([18]crown-6)(thf)$_2$][(^{Dipp}BIAN)Fe(1,3-tBu$_2$C$_2$P$_2$)] (**7**, from tBuCP, Figure 4). **6** and **7** were isolated as dark blue or violet crystals in 70% and 50% yield, respectively. The bond metrical data for both complexes are very similar to the values obtained for the related cobalt complexes. However, and in contrast to the cobaltates, **6** and **7** are paramagnetic and, therefore, reveal broad resonances in their ^{1}H NMR spectra in the region from

−4 to +12 ppm (see the Supporting Information for spectra). The results of magnetic susceptibility, EPR and ^{57}Fe Mössbauer measurements are discussed in the section *Electronic Structure Analysis* (see below).

Reactivity studies

Having substantial quantities of the 1,2- and 1,3-tBu$_2$C$_2$P$_2$ cobaltates **4** and **5** in hand, reactions of these complexes with different electrophiles were conducted, to examine differences in their reactivities. Reactions of the 1,3-isomer **5** with HCl, Me$_3$SiCl and Cy$_2$PCl afforded only crystals of the neutral, partly deligated complex [(^{Dipp}BIAN)Co(μ-Cl)]$_2$ (see Supporting Information for molecular structure). However, we were able to detect a singlet signal in the ^{31}P{^{1}H} NMR spectrum at 194.2 ppm in some of these reactions. In reactions of **4** with HCl, MeI, Me$_3$SiCl and Ph$_2$PCl, this species was also formed and identified as [{(^{Dipp}BIAN)Co}$_2$(μ-η^4:η^4-1,2-tBu$_2$C$_2$P$_2$)] (**8**, Scheme 4, Figure 5), a neutral complex featuring a μ-bridging 1,2-diphosphacyclobutadiene ligand. This compound was also identified as a product in the reaction of **5** with Me$_3$SiCl and MeI and represents another example of 1,3-tBu$_2$C$_2$P$_2$ to 1,2-tBu$_2$C$_2$P$_2$ ligand isomerisation. Bridging diphosphacyclobutadiene complexes are scarce, and this is the first example of the 1,2-isomer being isolated in such a bridging coordination mode. Dinuclear complex **8** could plausibly form from the reaction of 0.5 equivalents of the bridging chlorido complex [(^{Dipp}BIAN)Co(μ-Cl)]$_2$ (formed as an intermediate, see above) with one equivalent of **4** and concomitant elimination of KCl. Regardless, due to difficulties in isolating [(^{Dipp}BIAN)Co(μ-Cl)]$_2$, this hypothesis has not yet been confirmed experimentally.

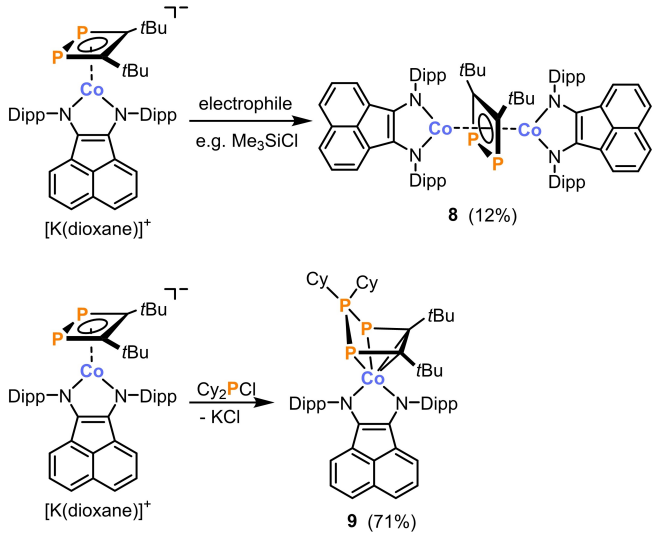

Scheme 4. Synthesis of complexes **8** (top) and **9** (bottom) by reactions of **4** with electrophiles.

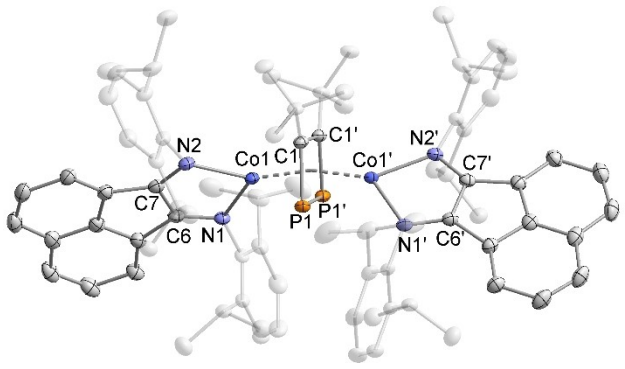

Figure 5. Molecular structure of **8** in the solid state.[31] Thermal ellipsoids are set at the 50% probability level. Hydrogen atoms are omitted for clarity. Selected bond lengths [Å] and angles [°]: P1–P1′ 2.3417(8), P1–C1 1.8602(16), C1–C1′ 1.449(3), N1–C6 1.327(2), N2–C7 1.334(2), C6–C7 1.425(2), Co1–N1 1.9287(14), Co1–N2 1.9874(14), Co-($C_2P_2^{centroid}$) 1.791(2), Co1···Co1′ 3.5547(5), C1–P1–P1′ 75.95(5), C1–C1′ P1–103.61(5).

Complex **8** was isolated in 12% yield using **4** as starting material and Me$_3$SiCl as electrophile and characterised by X-ray crystallography and elemental analysis as well as NMR and UV/Vis spectroscopy. The solid-state molecular structure of **8** reveals a long P1–P1′ bond (2.3417(8) Å), two slightly elongated P1–C1 bonds (1.8602(16) Å) and a C1–C1′ bond length (1.449(3) Å) that compares well to complexes **4** and **5**. The Co1···Co1′ distance of 3.5547(5) Å suggests no significant interaction between the metal atoms. The bond metric data of the BIAN ligand allows for a classification as monoanionic BIAN$^-$ (C6–C7 1.425(2) Å, N1–C6 1.327(2) Å, N2–C7 1.334(2) Å; cf. C–C 1.446(2) Å and C–N 1.3239(18) and 1.3326(19) Å in Na^{Dipp}BIAN).[18] A detailed discussion of the oxidation state of the BIAN ligand is given in the section *Electronic Structure Analysis*. Complex **8** is diamagnetic and features a ^{31}P{^{1}H} NMR singlet at a chemical shift of 194.2 ppm. The UV/Vis spectrum shows absorption bands at 620 and 830 nm, accounting for its dark blue colour in solution.

The reaction of Cy$_2$PCl with **4** and **5** revealed the particular synthetic utility of **4**. The neutral complex [(^{Dipp}BIAN)Co(η^4-tBu$_2$C$_2$P$_3$Cy$_2$)] (**9**), featuring an expanded 1,2,3-triphospholium ligand, was obtained upon insertion of a PCy$_2$ fragment into the P–P bond of **4** (Scheme 4). In case of **5**, this reaction was unselective giving rise to several signals in the ^{31}P{^{1}H} NMR spectrum (see Figure S19, Supporting Information). Even though substituted C$_2$P$_3$ rings are known (e.g. tri-organo P1,P2,P3-substituted triphospholenes), the motif of diorgano-substitution of P2 of a triphospholium ligand has not been reported to date.[19]

The solid-state molecular structure of **9** reveals η^4-coordination of the tBu$_2$C$_2$P$_3$Cy$_2$-ligand with P–P bond lengths (P1–P3 2.1549(6) Å, P2–P3 2.1535(6) Å) in the range commonly observed for P–P single bonds (Figure 6).[20] The structural parameters indicate the presence of a monoanionic BIAN$^-$ ligand (C1–C2 1.447(3) Å, N1–C11 1.347(2) Å, N2–C12 1.338(2) Å).[18] Complex **9** was isolated in 71% yield as dark blue crystals and is diamagnetic in solution as revealed by sharp resonances for the ^{Dipp}BIAN ligand and the tBu and Cy groups. The ^{31}P{^{1}H} NMR spectrum shows two signals: a doublet at −90.3 ppm ($^1J_{PP}$ = 349.6 Hz), corresponding to the three-coordinate P-atoms, and a coupled triplet resonance at 55.5 ppm, which can be assigned to the tetracoordinate P atom. The blue

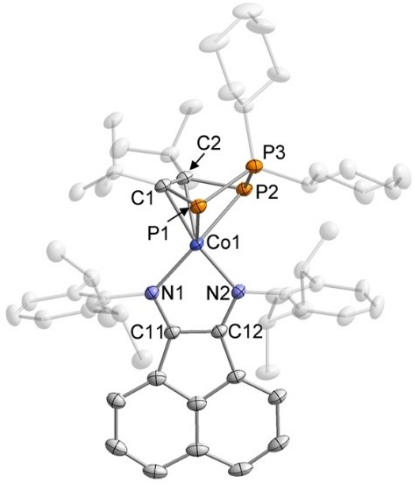

Figure 6. Molecular structure of **9** in the solid state.[31] Thermal ellipsoids are set at the 50% probability level. Hydrogen atoms and solvent of crystallisation are omitted for clarity. Selected bond lengths [Å] and angles [°]: Co1–P1 2.3049(5), Co1–P2 2.2643(5), Co1–C1 2.1070(18), Co1–C2 2.1041(18), Co1–N1 1.9850(15), Co1–N2 1.9046(15), P1–P3 2.1549(6), P2–P3 2.1535(6), P1–C1 1.8431(18), P2–C2 1.8147(19), C1–C2 1.447(3), N1–C11 1.347(2), N2–C12 1.338(2), C12–C11 1.406(3), C1–P1–P3 91.24(6), C2–P2–P3 93.38(6), P2–P3–P1 90.79(2), C2–C1–P1 117.67(13), C1–C2–P2 114.91(13).

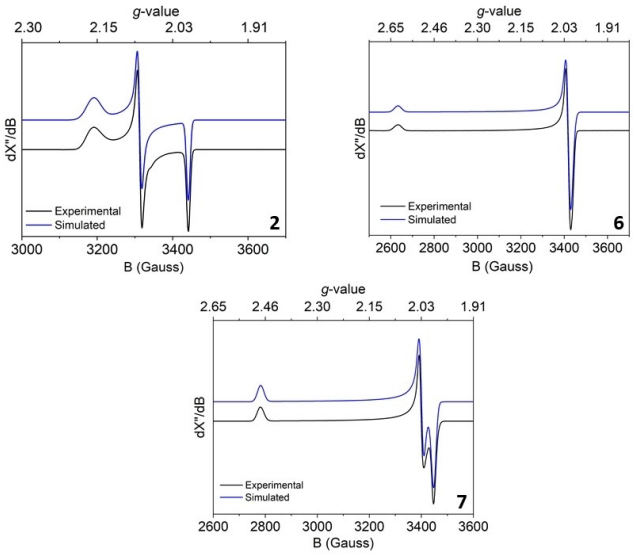

Figure 7. Experimental and simulated X-band EPR spectrum of **2** (top left), **6** (top right) and **7** (bottom) in a 2-methyl-THF glass. **2**: temperature: 10 K, Freq.: 9.646813 GHz, power: 0.2000 mW, mod. amp: 3.000 Gauss; g-tensor parameters obtained from simulations are: $g_{11}=2.161$, $g_{22}=2.081$, $g_{33}=2.003$, 1.10 mT Gaussian line width, 0.029 MHz g_{33}-strain; **6**: temperature: 20 K, Freq.: 9.642478 GHz, power: 0.6325 mW, mod. amp: 1.000 Gauss; g-tensor parameters obtained from simulations are: $g_{11}=2.617$, $g_{22}=2.015$, $g_{33}=2.007$; **7**: temperature: 20 K, Freq. : 9.646713 GHz, power: 0.6325 mW, mod. amp: 4.000 Gauss; g-tensor parameters obtained from simulations are: $g_{11}=2.478$, $g_{22}=2.027$, $g_{33}=1.999$.

colour of **9** can be attributed to two intense absorption bands in the UV/Vis spectrum at 560 and 660 nm.

Electronic structure analysis

Several spectroscopic and quantum chemical methods were employed in order to analyse the electronic structure of the complexes described herein. We were especially interested in the physical oxidation states of the metal atoms. Therefore, the bond lengths in all BIAN-containing complexes were analysed using the recently developed protocol for diazabutadiene-based ligands.[21] This method is based on a statistical analysis of bond metric data obtained from X-ray crystallography and can be used to determine a (non-integer) metrical oxidation state of the ligands and eventually the metal atom. However, BIAN ligands deviate structurally significantly from diazadiene ligands due to their aromatic backbone. Hence, the metrical oxidation state (MOS) model is expected to underestimate the bond lengths for reduced BIAN ligands and, therefore, further investigations on the complexes' electronic structure were conducted by spectroscopic analysis and quantum chemical calculations.

First, X-band EPR spectra of paramagnetic species (**2**, **6** and **7**) were recorded at 10 and 20 K, revealing rhombic spectra for all systems investigated without any resolved hyperfine features (see Figure 7). The spectra were simulated and the obtained *g*-values are given in Table 1; these *g*-values point towards a single metal-centred unpaired electron ($S=^1/_2$ spin system); thus, implying low-spin Fe(I) or Fe(III) complexes. The *g*-tensors were also calculated at the CASSCF-NEVPT2/DKH-def2-TZVP level of theory for the anionic complexes

Table 1. EPR spectroscopic parameters for compounds **2**, **6**/**6′** and **7**/**7′**.

Compound		g_{11}	g_{22}	g_{33}
2	Exp.	2.161	2.081	2.003
	Calc.	2.203	2.107	2.008
6	Exp.	2.617	2.015	2.007
6′	Calc.	2.600	2.004	1.997
7	Exp.	2.478	2.027	1.999
7′	Calc.	2.404	2.015	1.993

[Fe(1,2-*t*Bu$_2$C$_2$P$_2$)(anthracene)]$^-$ (**2**), [(^{Dmp}BIAN)Fe(1,2-*t*Bu$_2$C$_2$P$_2$)]$^-$ (**6′**) and [(^{Dmp}BIAN)Fe(1,3-*t*Bu$_2$C$_2$P$_2$)]$^-$ (**7′**).[22] The values obtained from these calculations for all compounds are in good agreement with the experimental values, suggesting that the calculated electronic structure fits the experimentally observed structure.

Next, the solution magnetic moments of **2**, **6** and **7** in THF-d$_8$ were determined using the Evans NMR method. A magnetic moment of 1.9(1) μ_B was measured for **2**, which is close to the spin-only value for a $S=^1/_2$ ground state ($\mu_{eff}^{spin-only}=1.73$). Accordingly, the magnetic moments of **6** and **7** were determined as $\mu_{eff}=2.0(1)$ μ_B in both cases. These values are consistent with low-spin Fe(I) and Fe(III) systems.

The zero-field ^{57}Fe Mössbauer spectra of [K([18]crown-6)][Fe(1,2-*t*Bu$_2$C$_2$P$_2$)(anthracene)] (**2**), [K([18]crown-6)(1,4-dioxane)][(^{Dipp}BIAN)Fe(1,2-*t*Bu$_2$C$_2$P$_2$)] (**6**) and [K([18]crown-6)(thf)$_2$][(^{Dipp}BIAN)Fe(1,3-*t*Bu$_2$C$_2$P$_2$)] (**7**) are shown in Figure 8. These spectra show the presence of a single species with an

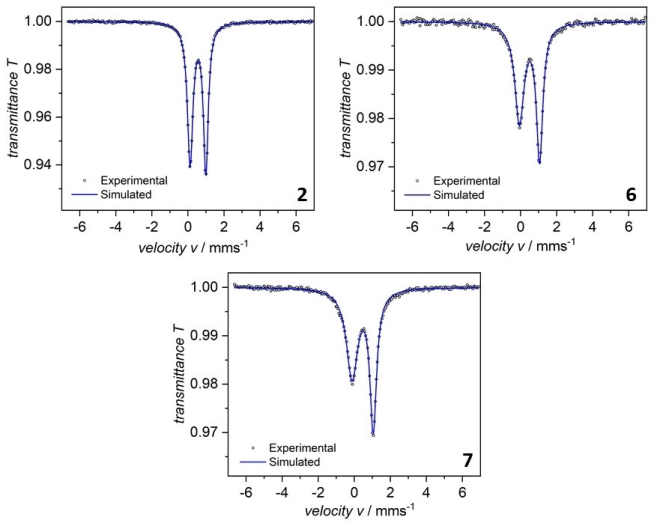

Figure 8. Experimental and simulated zero-field ^{57}Fe Mössbauer spectra of solid samples of **2** (top left), **6** (top right) and **7** (bottom) recorded at 77 K.

integral fit of the transmission in each case. The corresponding fitting parameters are listed in Table 2.

The isomer shifts, δ, range from 0.46 (**7**) to 0.55 mm·s^{-1} (**2**). The quadrupole splittings, ΔE_Q, of **6** and **7** are similar (1.12 and 1.18 mm·s^{-1}, respectively), while the value obtained for **2** differs (0.87 mm·s^{-1}). The isomer shifts and quadrupole splittings of the related complexes [K([18]crown-6)][Cp*Fe(anthracene)] (Cp* = C_5Me_5; $\delta = 0.56$ mm·s^{-1}, $\Delta E_Q = 2.56$ mm·s^{-1}, T = 78 K), [K([18]crown-6)(thf)$_2$][Fe(1,3-tBu$_2$C$_2$P$_2$)$_2$] ($\delta = 0.431$ mm·s^{-1}, $\Delta E_Q = 1.16$ mm·s^{-1}, T = 85 K)[23] and [K([18]crown-6)(thf)$_{0.2}$][(^{Dipp}BIAN)Fe(1,5-cod)] ($\delta = 0.23$ mm·s^{-1}, $\Delta E_Q = 2.26$ mm·s^{-1}, T = 80 K) have been reported previously.[24–26] A comparison reveals that the isomer shift of the 1,2-diphosphacyclobutadiene iron complexes (**2** and **6**) are comparable to [K([18]crown-6)][Cp*Fe(anthracene)], whereas the 1,3-diphosphacyclobutadiene complex **7** compares best to the homoleptic complex [K([18]crown-6)(thf)$_2$][Fe(1,3-tBu$_2$C$_2$P$_2$)$_2$]. This comparison reveals that the iron centre in **7** has a lower electron density than in the isomeric complex **6** (Table 2), suggesting that the acceptor strength of the 1,2-diphosphacyclobutadiene ligand is higher compared to its 1,3-isomer. As shown in Table 2, the quadrupole splittings were well reproduced by CASSCF calculations. Moreover, the electron densities on the iron nuclei of all complexes were calculated, giving a similar trend as the isomer shifts. As such, the electron density at the iron atom in **2** is the lowest, which is in agreement with its rather high (positive) isomer shift.

Finally, analysis of the localised occupied orbitals in [(^{Dmp}BIAN)Co(1,2-tBu$_2$C$_2$P$_2$)]$^-$ (**4′**, Figure 9) and [(^{Dmp}BIAN)Co(1,3-tBu$_2$C$_2$P$_2$)]$^-$ (**5′**) [see the Supporting Information for a depiction] – obtained by CASSCF calculations – shows the presence of two lone pairs on the N-atoms of the ^{Dmp}BIAN ligand as well as a double bond for the C11–C12 bond. In addition, the Mayer bond indices in the ^{Dmp}BIAN complexes **4′**, **5′**, **6′** and **7′** for the N1–C11 and N2–C12 bonds are close to the values of single bonds (ranging from 1.13 to 1.29), whereas the values for the C11–C12 bonds range from 1.95 to 2.07, providing further evidence for the presence of a C=C double bond. Hence, the computational analyses indicate that the dianionic form BIAN^{2-} is likely present in our complexes. This is in contrast to the MOS analysis derived from crystallography, which implied monoanionic BIAN$^-$ ligands (see above), but is in line with the Mössbauer spectroscopic data.

Further analysis of the CASSCF natural orbitals shows that the tBu$_2$C$_2$P$_2$ ligands form highly covalent bonds to the metal centre for complexes **4′**, **5′**, **6′**, **7′** and [Fe(1,2-tBu$_2$C$_2$P$_2$)(anthracene)]$^-$ (see Figures S38–S42, Supporting Information). Such high covalency has been observed in previous DFT studies on the electronic structure of 1,3-diphosphacyclo-

Table 2. ^{57}Fe Mössbauer spectroscopic parameters for compounds **2**, **6** and **7**.

Compound		Δ[a] [mm·s^{-1}]	P[b] [a.u.]	$\lvert\Delta E_Q$[c]$\rvert$ [mm·s^{-1}]	Γ_{fwhm}[d] [mm·s^{-1}]
2	Exp.	0.55		0.87	0.37
	Calc.		11810.059	0.98	
6	Exp.	0.50		1.12	0.62
	Calc.		11810.099	1.08	
7	Exp.	0.46		1.18	0.76
	Calc		11810.475	1.20	

[a] Isomer shift, [b] Calculated electron density at the nucleus (arbitrary unit, CASSCF), [c] Experimentally determined and calculated (CASSCF) quadrupole splittings, [d] Full width at half maximum.

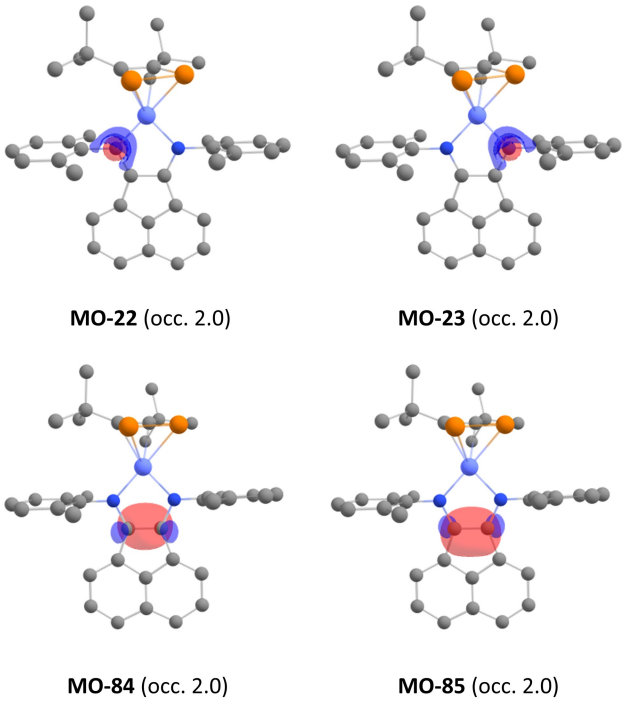

Figure 9. Selected localised molecular orbitals below the active space of a CASSCF calculation [RIJCOSX/TZVP-def2/JK, CP(PPP) on Co] on [(^{Dmp}BIAN)Co(1,2-tBu$_2$C$_2$P$_2$)]$^-$. The occupancy of each orbital is given in parentheses (2.0). Isosurface value for MO-22 and MO-23: 0.0075; for MO-84 and MO-85: 0.06.

butadiene complexes and makes the assignment of an oxidation state to the metal centres ambiguous.[25] Overall, and considering the presence of BIAN^{2-}, the bonding scenario can be described as being intermediate between two extreme cases, namely a neutral π-accepting tBu$_2$C$_2$P$_2$ ligand and a low-spin metal(I) centre or a dianionic π-donating tBu$_2$C$_2$P$_2$ ligand and a low-spin metal(III) centre.

Conclusion

In summary, we have shown that the recently reported mixed tetrahedrane (tBuCP)$_2$ (**1**) acts as a reliable source of previously difficult-to-access 1,2-diphosphacyclobutadiene ligands in reactions with cobalt and iron metalates. While these 1,2-isomers are available by P–C bond cleavage of the C$_2$P$_2$ tetrahedron, the corresponding 1,3-isomers are also available by head-to-tail cyclodimerisation of tBuCP upon reaction with the same metalates. In this manner it has been possible to rapidly prepare a family of iron and cobalt complexes, including both homoleptic and heteroleptic examples. Such convenient access to both isomers has permitted direct comparative studies of their reactivity, establishing clear differences in the behaviour of the 1,2- and 1,3-complexes. These have revealed the particular utility of 1,2-diphosphacyclobutadiene complexes for further transformations, as exemplified by unprecedented preparations of both an diorgano-substituted triphospholium ligand and a tBu$_2$C$_2$P$_2$ ligand in a μ-η^4:η^4-coordination mode. Further reactivity studies on the use of the new metalates in synthesis and catalysis are ongoing.

Experimental Section

General synthetic methods

All reactions and product manipulations were carried out in flame-dried glassware under an inert atmosphere of argon using standard Schlenk-line or glovebox techniques (maintained at <0.1 ppm H$_2$O and <0.1 ppm O$_2$). [K(thf)$_{0.2}$][Co(η^4-cod)$_2$],[27] [K([18]crown-6)][Fe(anthracene)$_2$],[28] [K(dme)$_2$][Co(anthracene)$_2$],[29] [K(thf)$_{1.5}$][(^{Dipp}BIAN)Co(η^4-cod)],[12] [K([18]crown-6)][(^{Dipp}BIAN)Fe(η^4-cod)],[26] (tBuCP)$_2$[5] and tBuCP[30] were prepared according to previously reported procedures. All other chemicals were purchased from commercial suppliers and used without further purification. Solvents were dried and degassed with a MBraun SPS800 solvent purification system. All dry solvents except *n*-hexane were stored under argon over activated 3 Å molecular sieves in gas-tight ampules. *n*-Hexane was instead stored over a potassium mirror.

General Analytical Techniques

NMR spectra were recorded on Bruker Avance 300 or 400 spectrometers at 300 K, unless otherwise noted, and internally referenced to residual solvent resonances (^{1}H NMR: THF-d$_8$: 1.72 ppm, C$_6$D$_6$: 7.16 ppm, ^{13}C{^{1}H} NMR: THF-d$_8$: 25.31 ppm, C$_6$D$_6$: 128.06 ppm). Chemical shifts δ are given in ppm referring to external standards of tetramethylsilane (^{1}H, ^{13}C{^{1}H}), 85% phosphoric acid (^{31}P and ^{31}P{^{1}H} spectra). ^{1}H and ^{13}C NMR signals were assigned based on 2D NMR spectra (^{1}H,^{1}H-COSY, ^{1}H,^{13}C-HSQC, ^{1}H,^{13}C-HMQC).

UV/Vis electronic absorption spectra were recorded on an Ocean Optics Flame Spectrometer. Diluted solutions of the complexes in THF were prepared in the following concentrations: $5.9\cdot10^{-5}$ M (**2**), $3.8\cdot10^{-5}$ M (**4**), $1.8\cdot10^{-5}$ M (**5**), $3.2\cdot10^{-5}$ M (**6**), $3.5\cdot10^{-5}$ M (**7**), $4.5\cdot10^{-5}$ M (**8**), $6.3\cdot10^{-5}$ M (**9**). CHN combustion elemental analyses were performed by the central analytics department of the University of Regensburg. Details on single crystals X-ray crystallography are given in the Supporting Information.

Synthesis of compounds

[K([18]crown-6)][Fe(1,2-tBu$_2$C$_2$P$_2$)(anthracene)] (2)

To a deep red, cold (−80 °C) solution of [K([18]crown-6)][Fe(anthracene)$_2$] (1053.4 mg, 1.23 mmol, 1.0 eq.) was added (tBuCP)$_2$ (3.0 mL, c = 0.5 M in toluene, 1.47 mmol, 1.2 eq.). After stirring overnight and allowing the solution to warm to ambient temperature, a colour change to deep green was observed. Subsequently, the solvent was removed and the dark green residue was dried *in vacuo*. The residue was washed with *n*-hexane (30 mL) and benzene (30 mL) and dried *in vacuo*. After extraction with THF (10 mL), the deep green solution was layered with *n*-hexane (60 mL). Slow diffusion over 3 days at ambient temperature afforded green blocks of [K([18]crown-6)][Fe(1,2-tBu$_2$C$_2$P$_2$)(anthracene)] (**2**), which were isolated by decanting the supernatant and dried *in vacuo*. These crystals still contain residual benzene (Figure S1), which can be removed upon grinding the sample and further drying *in vacuo*. Single crystals suitable for X-ray diffraction were obtained by slow diffusion of *n*-hexane into a saturated solution of **2** in benzene.

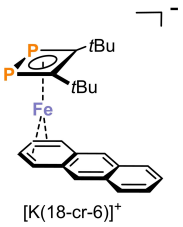

C$_{36}$H$_{52}$FeKO$_6$P$_2$, MW = 737.70 g·mol^{-1}, yield: 760 mg (84%). ^{1}H NMR (400 MHz, 300 K, THF-d$_8$) No signal was observed in the range −150–150 ppm. Evans NMR: μ = 1.9(1) μ$_B$. ^{31}P{^{1}H} NMR (162 MHz, 300 K, C$_6$D$_6$) No signal was observed in the range −150–150 ppm. Elemental Analysis calcd. C 58.61, H 7.11; found C 59.33, H 7.20. UV/Vis (THF): λ_{max} (nm, ε_{max}/L·mol^{-1}·cm^{-1}) 330 (19 000), 440 (7 000), 650 (6 000).

[K(1,4-dioxane)][(^{Dipp}BIAN)Co(1,2-tBu$_2$C$_2$P$_2$)] (4)

To a solution of [K(thf)$_{1.5}$][(^{Dipp}BIAN)Co(η^4-cod)] (250 mg, 0.32 mmol, 1.0 eq) in THF (5 mL) was added (tBuCP)$_2$ (1.2 mL, c = 0.4 M in toluene, 0.48 mmol, 1.5 eq.). The deep green solution was stirred at ambient temperature for three days whilst turning turquoise. Subsequently, the solvent was removed *in vacuo* and the residue was washed with *n*-hexane (15 mL) and extracted with 1,4-dioxane (20 mL). The solution was concentrated to ca. 5 mL and layered with *n*-hexane (30 mL). Storage at room temperature for 5 days afforded deep turquoise crystals of [K(1,4-dioxane)][^{Dipp}BIANCo(1,2-tBu$_2$C$_2$P$_2$)] (**4**). The supernatant was decanted and the crystals were dried *in vacuo*. Elemental analysis and the ^{1}H and ^{13}C{^{1}H} NMR spectra indicate that the 1,4-dioxane molecule remains in the crystalline solid after drying.

Crystals suitable for X-ray crystallography were grown by slow diffusion of *n*-hexane into a saturated solution of **4** in 1,4-dioxane at ambient temperature.

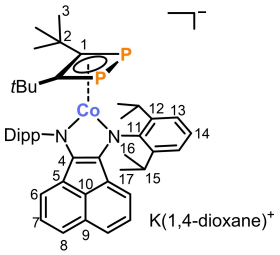

$C_{50}H_{66}CoKN_2O_2P_2$, MW = 887.07 g·mol^{-1}, yield: 180 mg (63 %). ^{1}H NMR (400 MHz, 300 K, THF-d$_8$) δ = 0.81 (d, $^3J_{HH}$ = 6.7 Hz, 12H, C^{16}H), 1.10 (s, 18H, C^{3}H), 1.27 (d, $^3J_{HH}$ = 6.8 Hz, C^{17}H), 3.55 (s, 8H, 1,4-dioxane), 4.71 (sept, $^3J_{HH}$ = 6.7 Hz, 4H, C^{15}H), 4.99 (d, $^3J_{HH}$ = 7.0 Hz, 2H, C^{6}H), 6.42 (pseudo-t, $^3J_{HH}$ = 7.6 Hz, 2H, C^{7}H), 6.61 (d, $^3J_{HH}$ = 8.2 Hz, 2H, C^{8}H), 7.14 (m, 6H, C^{13+14}H) ppm. ^{13}C{^{1}H} NMR (100 MHz, 300 K, THF-d$_8$) δ = 24.8 (s, C^{17}, overlapping with THF-signal), 26.2 (s, C^{16}), 29.0 (s, C^{15}), 33.0 (s, C^3), 37.0 (s, C^2), 67.3 (s, C$^{1,4-dioxane}$, overlapping with THF signal), 105.2 (br s, C^1), 116.7 (s, C^6), 119.6 (s, C^8), 123.3 (s, C^{13}), 123.8 (s, C^{14}), 127.7 (s, C^7), 129.5 (s, C^9), 136.1 (s, C^5), 137.3 (s, C^{10}), 142.5 (s, C^{12}), 150.2 (s, C^4), 161.6 (s, C^{11}) ppm. ^{31}P{^{1}H} NMR (162 MHz, 300 K, THF-d$_8$) δ = −121.8 (s) ppm. Elemental Analysis calcd. C 67.70, H 7.50, N 3.16; found C 67.63, H 7.45, N 3.01. UV/Vis (THF): λ_{max} (nm, ε_{max} /L·mol^{-1}·cm^{-1}) 270 (17 000), 380 (5 400sh), 630 (22 000).

[K(thf)$_3$][(^{Dipp}BIAN)Co(1,3-tBu$_2$C$_2$P$_2$)] (5)

A solution of *t*BuCP (0.18 mL, c = 3.2 M in TMS$_2$O, 0.58 mmol, 2.1 eq) was added dropwise to a cold (−30 °C) solution of [K(thf)$_{1.5}$][(^{Dipp}BIAN)Co(η^4-cod)] (200 mg, 0.27 mmol, 1.0 eq) in THF (5 mL). The green solution turned turquoise immediately and was stirred for 18 h at ambient temperature. After removal of the solvent *in vacuo*, the residue was washed with *n*-hexane (5 mL) and extracted with THF (3.0 mL). Layering the solution with *n*-hexane (15 mL) and storage at room temperature afforded deep turquoise crystals of [K(thf)$_3$][Co(^{Dipp}BIAN)(1,3-*t*Bu$_2$C$_2$P$_2$)]. The supernatant was decanted and the crystals were dried *in vacuo*. Elemental analysis and the ^{1}H and ^{13}C{^{1}H} NMR spectra indicate that three THF molecules remain in the crystalline solid after drying. Crystals suitable for X-ray crystallography were grown by slow diffusion of *n*-hexane into a saturated solution of [K(thf)$_3$][Co(^{Dipp}BIAN)(1,3-*t*Bu$_2$C$_2$P$_2$)] in THF at ambient temperature.

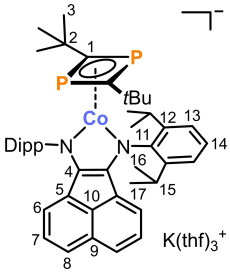

$C_{58}H_{82}CoKN_2O_3P_2$, MW = 1015.28 g·mol^{-1}, yield: 175 mg (64 %). ^{1}H NMR (400 MHz, 300 K, THF-d$_8$) δ = 0.80 (br m, 12H, C$^{16/17}$H), 0.93 (br s, 18H, C^{3}H), 1.33 (br m, 12H, C$^{16/17}$H), 5.00 (br m, 6H, C^{15}H/CH^{BIAN}), 6.36 (br m, 2H, CH^{BIAN}), 6.61 (br m, 2H, CH^{BIAN}), 7.14 (br m, 6H, C$^{13/14}$H) ppm. ^{13}C{^{1}H} NMR (100 MHz, 300 K, THF-d$_8$) δ = 25.2 (s, C$^{16/17}$), 26.4 (s, C$^{16/17}$), 28.7 (s, C^2), 32.5 (t, $^3J_{PC}$ = 4.9 Hz, C^3), 34.3 (t, $^2J_{PC}$ = 6.6 Hz, C^2), 89.4 (t, $^1J_{PC}$ = 49.5 Hz, C^1), 116.4 (s, C$^{4-10}$), 119.3 (s, C$^{4-10}$), 123.4 (s, C$^{13/14}$), 123.5 (s, C$^{13/14}$), 127.5 (s, C$^{4-10}$), 128.9 (s, C$^{4-10}$), 136.1 (s, C$^{4-10}$) 137.3 (s, C$^{4-10}$), 143.5 (s, C$^{4-10}$), 146.9 (s, C^{12}), 160.5 (s, C^{11}) ppm. ^{31}P{^{1}H} NMR (162 MHz, 300 K, THF-d$_8$) δ = 1.8 (s) ppm. Elemental Analysis calcd. C 68.62, H 8.14, N 2.76, found. C 68.63, H 7.96, N 2.60. UV/Vis (THF) λ_{max} (nm, ε_{max} /L·mol^{-1}·cm^{-1}): 294 (22800), 388 (6000), 605 (16700), 738 (7800).

[K([18]crown-6)(dioxane)][(^{Dipp}BIAN)Fe(1,2-tBu$_2$C$_2$P$_2$)] (6)

To a solution of [K([18]crown-6)(thf)$_2$][(^{Dipp}BIAN)Fe(η^4-cod)] (400 mg, 0.36 mmol, 1.0 eq) in THF (20 mL) was added (*t*BuCP)$_2$ (2.3 mL, c = 0.5 M in toluene, 1.14 mmol, 1.5 eq) at ambient temperature. The green solution turned dark blue after 10 minutes and was stirred at ambient temperature for 3 days. After removal of the solvent *in vacuo*, the residue was washed with *n*-hexane (50 mL) and extracted with 1,4-dioxane (200 mL). Subsequently, the solution was concentrated to ca. 50 mL and layered with *n*-hexane (400 mL). Storage at room temperature for 4 days afforded deep blue crystals of [K([18]crown-6)(1,4-dioxane)][Fe(^{Dipp}BIAN)(1,2-*t*Bu$_2$C$_2$P$_2$)] (**6**) The supernatant was decanted and the crystals were dried *in vacuo*. Elemental analysis and the ^{1}H and ^{13}C{^{1}H} NMR spectra indicate that the 1,4-dioxane molecule remains in the crystalline solid after drying. Crystals suitable for X-ray crystallography were grown by slow diffusion of *n*-hexane into a saturated solution of **6** in 1,4-dioxane at ambient temperature.

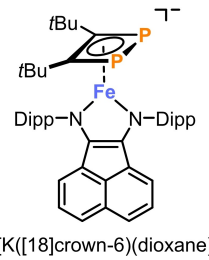

$C_{66}H_{98}FeKN_2O_{10}P_2$, MW = 1148.30 g·mol^{-1}, yield: 290 mg (70 %). ^{1}H NMR (400 MHz, 300 K, THF-d$_8$) δ = −3.9 (br s), 0.7 (br s), 2.7 (br s), 3.8 (s, 1,4-dioxane), 6.1 (br s), 7.7 (br s), 10.9 (br s) ppm. Evans NMR: μ = 2.0(1) μ$_B$. ^{31}P{^{1}H} NMR (162 MHz, 300 K, THF-d$_8$) No signal was observed in the range −150–150 ppm. Elemental Analysis calcd. C 64.85, H 7.90, N 2.44; found C 65.24, H 7.80, N 2.07. UV/Vis (THF): λ_{max} (nm, ε_{max} /L·mol^{-1}·cm^{-1}) 280 (30 000sh), 350 (16 000sh), 430 (9 000sh), 570 (14 000), 810 (14 000).

[K([18]crown-6)(thf)$_2$][(^{Dipp}BIAN)Fe(1,3-tBu$_2$C$_2$P$_2$)] (7)

A solution of *t*BuCP (0.22 mL, c = 3.5 M in TMS$_2$O, 0.28 mmol, 3.1 eq) was added dropwise to a cold (−30 °C) solution of [K([18]crown-6)(thf)$_2$][(^{Dipp}BIAN)Fe(η^4-cod)] (400 mg, 0.36 mmol, 1.0 eq) in THF (20 mL). The green solution turned deep violet immediately and was stirred for 18 h at ambient temperature. After removal of the solvent *in vacuo*, the residue was washed with *n*-hexane (20 mL) and extracted with THF (10 mL). Layering the solution with *n*-hexane (50 mL) and storage at room temperature afforded deep purple blocks of [K([18]crown-6)(thf)$_2$][Fe(^{Dipp}BIAN)(1,3-*t*Bu$_2$C$_2$P$_2$)]·THF. The supernatant was decanted and the crystals were dried *in vacuo*. Elemental analysis of the isolated, crystalline solid suggests a THF solvate with two K-coordinated and one additional THF molecule per formula unit. Crystals suitable for X-ray crystallography of the 1,4-dioxane containing salt [K([18]crown-6)(thf)$_{1.8}$(1,4-dioxane)$_{0.2}$][Fe(^{Dipp}BIAN)(1,3-*t*Bu$_2$C$_2$P$_2$)] were grown by slow diffusion of *n*-hexane into a saturated solution of **7** in THF at ambient temperature. Minor amounts of 1,4-dioxane originated from initial crystallisation attempts with this solvent.

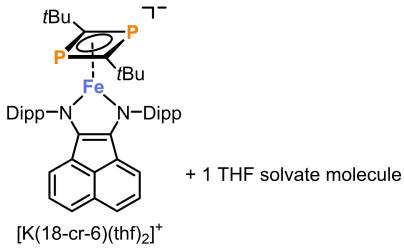

$C_{66}H_{98}FeKN_2O_8P_2 \cdot C_4H_8O$, MW = 1276.51 g·mol^{-1} (for **7** THF), yield: 180 mg (50%). ^{1}H NMR (400 MHz, 300 K, THF-d_8) δ = −3.5 (br s), −1.7 (br s), 2.2 (br s), 6.8 (br s), 7.9 (br s), 8.7 (br s), 10.6 (br s) ppm. Evans NMR: μ = 2.0(1) μ_B. ^{31}P{^{1}H} NMR (162 MHz, 300 K, THF-d_8) No signal was observed in the range −150–150 ppm. Elemental Analysis calcd. C 65.86, H 8.37, N 2.19; found C 65.92, H 8.09, N 2.09. UV/Vis (THF): λ_{max} (nm, ε_{max} /L·mol^{-1}·cm^{-1}) 290 (29 000), 370 (14 000sh), 540 (12 000), 800 (12 000).

[{(DippBIAN)Co}$_2$(μ-η^4:η^4-tBu$_2$C$_2$P$_2$)] (8)

To a solution of [K(1,4-dioxane)][DippBIANCo(1,2-*t*Bu$_2$C$_2$P$_2$)] (150 mg, 0.169 mmol, 1.0 eq) in THF (5 mL) at −80 °C was added Me_3SiCl (0.12 mL, c = 1.58 M in toluene, 0.19 mmol, 1.1 eq.). The solution was allowed to warm to room temperature within 18 h. During that time, the colour of the reaction solution changed from turquoise to dark blue. Subsequently, the solvent was removed *in vacuo* and the residue was extracted with *n*-hexane (5 mL). Storage at −30 °C for three days afforded dark blue crystals of [{(DippBIAN)Co}$_2$(μ-η^4:η^4-*t*Bu$_2$C$_2$P$_2$)]. The supernatant was decanted and the crystals were dried *in vacuo*. Crystals suitable for X-ray crystallography were grown by storing a saturated solution of [{(DippBIAN)Co}$_2$(μ-η^4:η^4-*t*Bu$_2$C$_2$P$_2$)] in *n*-hexane at ambient temperature overnight.

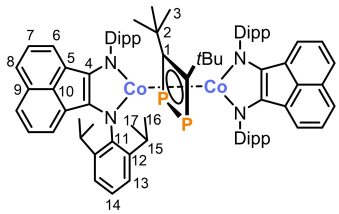

$C_{82}H_{98}Co_2N_4P_2$, MW = 1319.53 g·mol^{-1}, yield: 13 mg (12%). ^{1}H NMR (400 MHz, 300 K, C_6D_6) δ = 0.83 (d, $^3J_{HH}$ = 6.7 Hz, 24H, C^{16}H), 1.15 (s, 18H, C^{3}H), 1.20 (d, $^3J_{HH}$ = 6.7 Hz, C^{17}H), 3.7 (br s, 8H, C^{15}H), 6.55 (pseudo-t, $^3J_{HH}$ = 7.4 Hz, C^{7}H, overlapping with signal for C^{6}H), 6.58 (dd, $^3J_{HH}$ = 7.4 Hz, $^4J_{HH}$ = 1.2 Hz, C^{6}H), 7.11 (d, $^3J_{HH}$ = 7.8 Hz, C^{13}H), 7.38 (t, $^3J_{HH}$ = 7.8 Hz, C^{14}H), 7.89 (dd, $^3J_{HH}$ = 7.7 Hz, $^4J_{HH}$ = 1.1 Hz, C^{9}H) ppm. ^{13}C{^{1}H} NMR (100 MHz, 300 K, C_6D_6) δ = 24.5 (s, C^{17}), 25.8 (s, C^{16}), 28.7 (s, C^{15}), 31.5 (s, C^3), 37.7 (s, C^2), 119.1 (s, C^6), 122.9 (s, C^8), 124.1 (s, C^{13}), 126.8 (s, C^{14}), 130.1 (s, C^{10}), 131.2 (s, C^7), 135.7 (s, C^{12}), 136.3 (s, C^9), 142.8 (s, C^5), 159.3 (s, C^{11}), 162.7 (s, C^4) ppm (C^1 could not be detected; ^{1}H / ^{13}C{^{1}H} HMBC suggests a signal at ca. 113 ppm). ^{31}P{^{1}H} NMR (162 MHz, 300 K, C_6D_6) δ = 194.2 (s) ppm. Elemental Analysis calcd. C 74.64, H 7.49, N 4.25; found C 74.67, H 7.68, N 3.80. UV/Vis (THF): λ_{max} (nm, ε_{max} /L·mol^{-1}·cm^{-1}) 330 (22 000sh), 480 (9 500), 620 (20 700), 830 (14 500).

[(DippBIAN)Co(η^4-tBu$_2$C$_2$P$_3$Cy$_2$)] (9)

To a solution of [K(1,4-dioxane)][(DippBIAN)Co(1,2-*t*Bu$_2$C$_2$P$_2$)] (**4**, 85 mg, 0.096 mmol, 1.0 eq) in THF (3 mL) at −30 °C was added PCy_2Cl (0.9 mL, c = 0.11 M in *n*-hexane, 0.10 mmol, 1.0 eq.). The turquoise solution turned dark blue immediately. After stirring for 30 minutes at ambient temperature, the solvent was removed *in vacuo*. The residue was extracted with an *n*-hexane/toluene-mixture (10:1 v/v, 5 mL). Storage at −30 °C for three days afforded dark blue crystals of [(DippBIAN)Co(η^4-*t*Bu$_2$C$_2$P$_3$Cy$_2$)]. The supernatant was decanted and the crystals were dried *in vacuo*. The complex crystallises as a solvate with n-hexane and toluene according to ^{1}H and ^{13}C{^{1}H} NMR and elemental analysis. A solvent content of 1 toluene and 0.5 *n*-hexane molecules per formula unit was determined. Crystals suitable for X-ray crystallography were grown by storing a saturated solution of [(DippBIAN)Co(η^4-*t*Bu$_2$C$_2$P$_3$Cy$_2$)] in *n*-hexane at ambient temperature overnight.

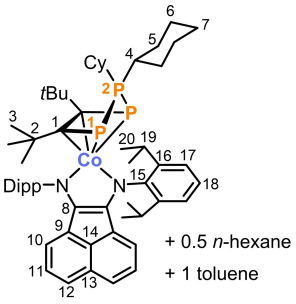

$C_{58}H_{80}CoN_2P_3 \cdot 0.5\ C_6H_{14} \cdot C_7H_8$, 1092.38 g·mol^{-1}, yield: 65 mg (62%). ^{1}H NMR (400 MHz, 300 K, C_6D_6) δ = 0.73-0.93 (m, 9H, C$^{5-7}$H + *n*-hexane), 0.97 (d, $^3J_{HH}$ = 6.5 Hz, 12H, C^{20}H), 1.13–1.63 (m, 19H, C$^{5-7}$H + *n*-hexane), 1.67 (d, $^3J_{HH}$ = 6.5 Hz, 12H, C^{20}H), 1.76 (s, 18H, C^{3}H), 4.31 (sept, $^3J_{HH}$ = 6.5 Hz, 4H, C^{19}H), 5.85 (d, $^3J_{HH}$ = 7.1 Hz, 2H, C^{10}H), 6.77 (pseudo-t, $^3J_{HH}$ = 8.1 Hz, 2H, C^{11}H), 7.27 (d, $^3J_{HH}$ = 8.1 Hz, 2H, C^{12}H), 7.33 (d, $^3J_{HH}$ = 7.2 Hz, 4H, C^{17}H), 7.42 (t, $^3J_{HH}$ = 7.2 Hz, 2H, C^{18}H) ppm. ^{13}C{^{1}H} NMR (100 MHz, 300 K, C_6D_6) δ = 25.2 (d, *J* = 4.5 Hz, C^{20}), 26.2 (m, C$^{4-7}$), 26.3 (s, C$^{20'}$), 27.1 (d, *J* = 9.5 Hz, C$^{4-7}$), 27.6 (d, *J* = 1.9 Hz, C$^{4-7}$), 29.0 (s, C^{19}), 30.4 (br s, C$^{4-7}$), 34.4 (dt, *J* = 24.1 Hz, 4.6 Hz, C$^{4-7}$), 36.8 (d, $^3J_{CP}$ = 14.5 Hz, C^3), 39.5 (d, $^2J_{CP}$ = 18.3 Hz, C^2), 40.9 (d, *J* = 16.4 Hz, C$^{4-7}$), 115.3 (m, C^1), 119.7 (s, C^{10}), 123.4 (s, C^{12}), 124.6 (s, C^{17}), 126.4 (s, C^{18}), 128.6 (s, C^{11}), 131.3 (s, C^{13}), 135.9 (s, C^9), 136.1 (s, C^{14}), 141.0 (s, C^{16}), 153.4 (s, C^8), 158.5 (s, C^{15}) ppm. ^{31}P{^{1}H} NMR (162 MHz, 300 K, C_6D_6) δ = −90.3 (d, $^1J_{PP}$ = 349.4 Hz, 2P, P^1), 55.5 (t, $^1J_{PP}$ = 349.6 Hz, 1P, P^2) ppm. Elemental Analysis calcd. C 74.77, H 8.77, N 2.56; found C 75.01, H 8.62, N 2.40. UV/Vis (THF): λ_{max} (nm, ε_{max} /L·mol^{-1}·cm^{-1}) 320 (17 000), 440 (9 300), 560 (12 000), 660 (12 500).

Acknowledgements

Financial support by the Deutsche Forschungsgemeinschaft (WO1496/10-1), the European Research Council (ERC CoG 772299), and the Fonds der Chemischen Industrie (Kekulé fellowships for G.H. and T.M.M.) is gratefully acknowledged. D.M.P. and K.M. acknowledge generous financial support from the Friedrich-Alexander-Universität Erlangen-Nürnberg (FAU). Open Access funding enabled and organized by Projekt DEAL.

Conflict of Interest

The authors declare no conflict of interest.

Keywords: phosphatetrahedranes · phosphaalkyne oligomers · phosphorus · iron · cobalt

[1] G. Maier, *Angew. Chem. Int. Ed. Engl.* **1988**, *27*, 309–332.
[2] G. Maier, S. Pfriem, U. Schäfer, R. Matusch, *Angew. Chem. Int. Ed. Engl.* **1978**, *17*, 520–521.
[3] A. R. Jupp, J. C. Slootweg, *Angew. Chem. Int. Ed.* **2020**, *59*, 10698–10700.
[4] a) S. C. Critchlow, J. D. Corbett, *Inorg. Chem.* **1982**, *21*, 3286–3290; b) S. C. Critchlow, J. D. Corbett, *Inorg. Chem.* **1985**, *24*, 979–981; c) G. C. W. Blase, *Z. Kristallogr. – Cryst. Mater.* **1991**, *196*, 207–211; d) L. Xu, S. C. Sevov, *Inorg. Chem.* **2000**, *39*, 5383–5389; e) F. Lips, I. Schellenberg, R. Pöttgen, S. Dehnen, *Chem. Eur. J.* **2009**, *15*, 12968–12973; f) F. Lips, M. Raupach, W. Massa, S. Dehnen, *Z. Anorg. Allg. Chem.* **2011**, *637*, 859–863; g) S. Gärtner, N. Korber, in *Zintl Ions: Principles and Recent Developments* (T. F. Fässler Editor) Springer-Verlag, Berlin, **2011**, pp. 28; h) S. Scharfe, F. Kraus, S. Stegmaier, A. Schier, T. F. Fässler, *Angew. Chem. Int. Ed.* **2011**, *50*, 3630–3670; i) U. Friedrich, M. Neumeier, C. Koch, N. Korber, *Chem. Commun.* **2012**, *48*, 10544–10546; j) R. Ababei, J. Heine, M. Hołyńska, G. Thiele, B. Weinert, X. Xie, F. Weigend, S. Dehnen, *Chem. Commun.* **2012**, *48*, 11295–11297; k) S. Mitzinger, L. Broeckaert, W. Massa, F. Weigend, S. Dehnen, *Nat. Commun.* **2016**, *7*, 10480; l) S. Mitzinger, J. Bandemehr, K. Reiter, J. S. McIndoe, X. Xie, F. Weigend, J. F. Corrigan, S. Dehnen, *Chem. Commun.* **2018**, *54*, 1421–1424; m) K. Mayer, J. Weßing, T. F. Fässler, R. A. Fischer, *Angew. Chem. Int. Ed.* **2018**, *57*, 14372–14393; n) R. J. Wilson, N. Lichtenberger, B. Weinert, S. Dehnen, *Chem. Rev.* **2019**, *119*, 8506–8554 .
[5] G. Hierlmeier, P. Coburger, M. Bodensteiner, R. Wolf, *Angew. Chem. Int. Ed.* **2019**, *58*, 16918–16922.
[6] a) M.-L. Y. Riu, R. L. Jones, W. J. Transue, P. Müller, C. C. Cummins, *Sci. Adv.* **2020**, *6*, eaaz3168; b) M.-L. Riu, A. K. Eckhardt, C. C. Cummins, *J. Am. Chem. Soc.* **2021**, 143, 13005–13009.
[7] G. Hierlmeier, R. Wolf, *Angew. Chem. Int. Ed.* **2021**, *60*, 6435–6440.
[8] a) I. Krossing, *J. Am. Chem. Soc.* **2001**, *123*, 4603–4604; b) E.-M. Rummel, P. Mastrorilli, S. Todisco, M. Latronico, G. Balázs, A. V. Virovets, M. Scheer, *Angew. Chem. Int. Ed.* **2016**, *55*, 13301–13305.
[9] G. Hierlmeier, M. K. Uttendorfer, R. Wolf, *Chem. Commun.* **2021**, *57*, 2356–2359.
[10] E. Urnėžius, W. W. Brennessel, C. J. Cramer, J. E. Ellis, P. v. R. Schleyer, *Science* **2002**, *295*, 832–834.
[11] a) E.-M. Schnöckelborg, J. J. Weigand, R. Wolf, *Angew. Chem. Int. Ed.* **2011**, *50*, 6657–6660; b) C. M. Hoidn, T. M. Maier, K. Trabitsch, J. J. Weigand, R. Wolf, *Angew. Chem. Int. Ed.* **2019**, *58*, 18931–18936.
[12] S. Pelties, T. Maier, D. Herrmann, B. de Bruin, C. Rebreyend, S. Gärtner, I. G. Shenderovich, R. Wolf, *Chem. Eur. J.* **2017**, *23*, 6094–6102.
[13] R. Wolf, A. W. Ehlers, J. C. Slootweg, M. Lutz, D. Gudat, M. Hunger, A. L. Spek, K. Lammertsma, *Angew. Chem. Int. Ed.* **2008**, *47*, 4584–4587.
[14] R. Wolf, J. C. Slootweg, A. W. Ehlers, F. Hartl, B. de Bruin, M. Lutz, A. L. Spek, K. Lammertsma, *Angew. Chem. Int. Ed.* **2009**, *48*, 3104–3107.
[15] a) J. Malberg, T. Wiegand, H. Eckert, M. Bodensteiner, R. Wolf, *Chem. Eur. J.* **2013**, *19*, 2356–2369; b) J. Malberg, M. Bodensteiner, D. Paul, T. Wiegand, H. Eckert, R. Wolf, *Angew. Chem. Int. Ed.* **2014**, *53*, 2771–2775; c) J. Malberg, T. Wiegand, H. Eckert, M. Bodensteiner, R. Wolf, *Eur. J. Inorg. Chem.* **2014**, 1638–1651; d) C. Rödl, R. Wolf, *Eur. J. Inorg. Chem.* **2016**, 736–742; e) C. Rödl, J. Bissmeyer neé Malberg, R. Wolf, *Z. Naturforsch. B* **2018**, *73*, 895–909; f) C. Rödl, K. Schwedtmann, J. J. Weigand, R. Wolf, *Chem. Eur. J.* **2019**, *25*, 6180–6188; g) C. Rödl, R. Wolf, *Chem. Eur. J.* **2019**, *25*, 8332–8343.
[16] E.-M. Rummel, G. Balázs, V. Heinl, M. Scheer, *Angew. Chem. Int. Ed.* **2017**, *56*, 9592–9596.
[17] a) P. Binger, G. Glaser, S. Albus, C. Krüger, *Chem. Ber.* **1995**, *128*, 1261–1265; b) F. W. Heinemann, S. Kummer, U. Seiss-Brandl, U. Zenneck, *Organometallics* **1999**, *18*, 2021–2029; c) A. D. Burrows, A. Dransfeld, M. Green, J. C. Jeffery, C. Jones, J. M. Lynam, M. T. Nguyen, *Angew. Chem. Int. Ed.* **2001**, *40*, 3221–3224; d) C. Jones, C. Schulten, A. Stasch, *Dalton Trans.* **2006**, 3733–3735; e) S. Deng, C. Schwarzmaier, M. Zabel, J. F. Nixon, M. Bodensteiner, E. V. Peresypkina, G. Balázs, M. Scheer, *Eur. J. Inorg. Chem.* **2011**, 2991–3001.
[18] I. L. Fedushkin, A. A. Skatova, V. A. Chudakova, G. K. Fukin, *Angew. Chem. Int. Ed.* **2003**, *42*, 3294–3298.
[19] a) T. L. Breen, D. W. Stephan, *Organometallics* **1997**, *16*, 365–369; b) H. G. Ang, S. G. Ang, X. Wang, *J. Chem. Soc. Dalton Trans.* **2000**, 3429–3434.
[20] a) P. Pyykkö, *J. Phys. Chem. A* **2015**, *119*, 2326–2337; b) P. Pyykkö, M. Atsumi, *Chem. Eur. J.* **2009**, *15*, 186–197.
[21] F. J. de Zwart, B. Reus, A. A. H. Laporte, V. Sinha, B. de Bruin, *Inorg. Chem.* **2021**, *60*, 3274–3281.
[22] a) F. Neese, *WIREs Comput. Mol. Sci.* **2012**, *2*, 73–78; b) F. Neese, *WIREs Comput. Mol. Sci.* **2018**, *8*, 8:e1327.
[23] Note that the Mössbauer spectrum of $[K([18]crown\text{-}6)(thf)_2][Fe(1,3\text{-}t\mathrm{Bu}_2\mathrm{C}_2\mathrm{P}_2)_2]$ was not recorded at 77 K. However, the isomer shift at 4.2 K (0.431 mms^{-1}) suggests that there is only a small difference upon further cooling down the sample.
[24] E.-M. Schnöckelborg, M. M. Khusniyarov, B. de Bruin, F. Hartl, T. Langer, M. Eul, S. Schulz, R. Pöttgen, R. Wolf, *Inorg. Chem.* **2012**, *51*, 6719–6730.
[25] R. Wolf, A. W. Ehlers, M. M. Khusniyarov, F. Hartl, B. de Bruin, G. J. Long, F. Grandjean, F. M. Schappacher, R. Pöttgen, J. C. Slootweg, M. Lutz, A. L. Spek, K. Lammertsma, *Chem. Eur. J.* **2010**, *16*, 14322–14334.
[26] T. M. Maier, M. Gawron, P. Coburger, M. Bodensteiner, R. Wolf, N. P. van Leest, B. de Bruin, S. Demeshko, F. Meyer, *Inorg. Chem.* **2020**, *59*, 16035–16052.
[27] K. Jonas, R. Mynott, C. Krüger, J. C. Sekutowski, Y.-H. Tsay, *Angew. Chem. Int. Ed. Engl.* **1976**, *15*, 767–768.
[28] W. W. Brennessel, R. E. Jilek, J. E. Ellis, *Angew. Chem. Int. Ed.* **2007**, *46*, 6132–6136.
[29] W. W. Brennessel, V. G. Young, J. E. Ellis, *Angew. Chem. Int. Ed.* **2002**, *41*, 1211–1215.
[30] G. Becker, G. Gresser, W. Uhl, *Z. Naturforsch. B* **1981**, *36*, 16–19.
[31] Deposition Numbers 2101038 (for **2**), 2101036 (for **3**), 2101043 (for **4**), 2101039 (for **5**), 2101037 (for **6**), 2101042 (for **7**), 2101040 (for **8**), 2101041 (for **9**), 2101044 (for $[(^{Dipp}BIAN)CoCl]_2$) contain the supplementary crystallographic data for this paper. These data are provided free of charge by the joint Cambridge Crystallographic Data Centre and Fachinformationszentrum Karlsruhe Access Structures service.

Manuscript received: June 29, 2021
Accepted manuscript online: August 23, 2021
Version of record online: September 27, 2021

